http://dx.doi.org/10.5012/bkcs.2014.35.8.2367

Synthesis and Biodistribution of Cat's Eye-shaped [^{57}Co]CoO@SiO_2 Nanoshell Aqueous Colloids for Single Photon Emission Computed Tomography (SPECT) Imaging Agent

Minjae Kwon,[†,‡] Jeong Hoon Park,[§] Beom-Su Jang,[§] and Hyun Jung[†,*]

[†]*Advanced Functional Nanohybrid Material Laboratory, Department of Chemistry, Dongguk University-Seoul Campus, Seoul 100-715, Korea. [*]E-mail: chemphile@dongguk.edu*
[‡]*Fire & Safety Evaluation Technology Center, Korea Conformity Laboratories, Chungcheongbuk-do 363-883, Korea*
[§]*ARTI, Korea Atomic Energy Research Institute (KAERI), Jeollabuk-do 580-185, Korea*
Received March 5, 2014, Accepted April 18, 2014

"Cat's eye"-shaped [^{57}Co]CoO@SiO_2 core-shell nanostructure was prepared by the reverse microemulsion method combined with radioisotope technique to investigate a potential imaging agent for a single photon emission computed tomography (SPECT) in nuclear medicine. The core cobalt oxide nanorods were obtained by thermal decomposition of Co-(oleate)$_2$ precursor from radio isotope Co-57 containing cobalt chloride and sodium oleate. The SiO_2 coating on the surface of the core cobalt oxide nanorods was produced by hydrolysis and a condensation reaction of tetraethylorthosilicate (TEOS) in the water phase of the reverse microemulsion system. *In vivo* test, micro SPECT image was acquired with nude mice after 30 min of intravenous injection of [^{57}Co]CoO@SiO_2 core-shell nanostructure.

Key Words : Cobalt, Nanoparticles, Silicate, Isotopic labeling, Imaging agents

Introduction

The field of molecular imaging has expanded tremendously over the last decade due to the visualization and measurement of biological pathway at cellular and molecular level in living system.[1] The imaging approaches include optical fluorescence, magnetic resonance imaging (MRI), computed tomography (CT), positron emission tomography (PET) and single photon emission computed tomography (SPECT).[2] Among these approaches, the radionuclide based imaging method such as SPECT and PET has advantages over other modalities because PET and SPECT are highly sensitive, quantitative, and limitless in tissue penetration.[3]

In recent, imaging agents for PET and SPECT were developed using nanotechnologies.[4] The use of nanoparticles as imaging agent has great potential for early detection, accurate diagnosis, and therapy of many diseases.[5] Nanoparticles which have size range from 1 to 100 nm show size-dependent physical and chemical properties.[6] Normally nanoparticles used in medical field can be categorized into inorganic, polymer and lipid nanoparticles.[7,8] Metal oxides such as iron oxide, cobalt oxide are probably one of the most interesting classes of inorganic nanoparticles because they form a wide variety of structures, and display many interesting properties and numerous applications.[9,10]

Cobalt oxide attracts attention as metalloradionuclides for imaging agent because Co-57 is radionuclide for SPECT.[11] There are two main radiolabeling methods for nanoparticles.[12] One is to label on the surface of nanoparticle directly. The other method is to label inside the nanoparticles. Both of them, radionuclide was conjugated with nanoparticles. In these cases, there is possibility that radionuclide was susceptible to cleavage on nanoparticles moiety by the various enzymes in living system thus it was hard to obtain effective imaging study. On the other hand, the radiolabelling method with metal oxide and the same metalloradionuclide overcomes this problem due to generation of radioactive nanoparticles themselves without cleavage. In this regard, core-shell structures by designing the Co-57 labeled nanoparticles as a core materials are suitable for bio-imaging applications.[13] Synthetic methods of uniformly nanosized cobalt oxide with high crystallinity, particular shapes and tunable sizes have been proposed using the thermal decomposition or sol-gel reaction.[14-16] One-dimensional cobalt oxide nanorods have much attention due to their unique properties from their dimensional anisotropy.[17]

For the biomedical application of cobalt oxide nanocrystals, the surface of oxide should be coated by suitable one such as natural polysaccharides, liposomes and synthetic polymers because of surface property and toxicity of cobalt oxide itself.[18] Among various coating materials, amorphous silica is commonly used as coating or encapsulating materials due to its hydrophilic nature and biocompatibility.[19] After silica coating on the core material, the surface properties of the core-shell nanostructure such as the charge, reactivity, stability, dispersibility and solubility of core materials can be controlled. Moreover, the hydroxyl group on silica shell can be easily modified with suitable functional molecules by simple hydrolysis and condensation reaction.[13]

In this study, we aim to develop a novel SPECT imaging agent using the Co-57 labeled CoO@SiO_2 core-shell nanostructures. The cat's eye-shaped CoO@SiO_2 core-shell nano-

structures were prepared by reverse microemulsion method in the presence of uniformly sized CoO nanorods. The physicochemical characterizations of the obtained CoO@SiO_2 core-shell nanostructure have been carried out, along with *in vivo* mice study by micro SPECT imaging diagnostics.

Experimental

Synthesis of the Core CoO Nanocrystals. 4.76 g of cobalt chloride hexahydrate and 12.18 g of sodium oleate were added to mixture solution (15 mL of ethanol, 20 mL of distilled water, and 35 mL of *n*-hexane). The mixture solution was heated to 70 °C for 4 h. After cooling, the upper Co-(oleate)$_2$ solution was washed using distilled water and dried in a vacuum. 6.24 g of the Co-(oleate)$_2$ was dissolved in 100 g of 1-octadecene. The solution was then heated to 320 °C with vigorous stirring. The reaction mixture was maintained at this temperature for 60 min to induce sufficient growth. After cooling the reaction solution, it was centrifuged and washed several times using a mixture of acetone and *n*-hexane. The resulting product was redispersed in cyclohexane.

Synthesis of the CoO@SiO_2 Nanoshell Aqueous Colloids. 915 μL mother solution of CoO cyclohexane solution was dispersed in 21 mL of cyclohexane contained 4.9 mL of polyoxyethylene nonylphenyl ether. The resulting mixture was sonicated for 1 h, and magnetic stirring for 12 h. Then, distilled water (46.4 μL) was added to mixture solution. Next, tetraethylorthosilicate (100 μL) and 3-aminopropyltrimethoxysilane (102.9 μL) were added and the reaction was continued for 36 h at room temperature. Finally, the CoO@SiO_2 nanoshell material was isolated by methanol, and redispersed in ethanol.

Radiolabeling. 3.04 g of sodium oleate was suspended in 9 mL of hexane and 4 mL of ethanol at 70 °C. Next, 1.19 g of cobalt chloride hexahydrate, 1 mCi [^{57}Co]$CoCl_2$ solution and 5 mL of distilled water were added. The mixture was heated to 70 °C for 4 h. After cooling, the upper Co-(oleate)$_2$ layer was washed with distilled water and dried in a vacuum. 2.49 g of the Co-(oleate)$_2$ was dissolved in 50 g of 1-octadecene. The mixture was then heated to 320 °C with magnetic stirring. The reaction solution was maintained at this temperature for 60 min to induce sufficient growth. After cooling, the obtained solution was centrifuged and washed with acetone until complete removal of unreacted radioactive species at washing solution. The silica coating process on Co-57 contained CoO was the same way that of CoO@SiO_2 nanoshell.

Single Photon Emission Computed Tomography Imaging of Mice. The mice were anesthetized with 2% isoflurane in 100% oxygen (positioned prone in the cradle). 100 μCi of [^{57}Co]CoO@SiO_2 was intravenously administrated in biodistribution. 100 μCi of Co-57 was converted to mass unit as following equation. 100 μCi of Co-57 was equal to 1.18 × 10^{-8} g.

$$\mathrm{A\ (Ci)} = \frac{1.13\times10^{13}\times \mathrm{W(g)}}{\mathrm{M(u)}\times \mathrm{T(s)}} \quad (1)$$

Eq. (1). Radioactivity was converted to mass: A (Curie), W (gram), M (atomic mass), T (half life time, second)

The micro SPECT image was acquired at 30 min after injection. The CT scans were used for the anatomical reference. For the CT scans, the X-ray sources were used at 300 μA, and 60 kV for 15 min (one shot per projection). The CT resolution was 200 μm, and the number of acquired projections was 180.

Sample Characterization. The crystal structures were characterized by powder X-ray diffraction (XRD) measurements using Ni filtered Cu K_α radiation (λ = 1.5418 Å, Rigaku) with a graphite diffracted beam monochromator. The functional groups of chemical component were confirmed by Fourier transform-infrared (FT-IR) spectroscopy. The morphology was investigated using high resolution-transmission electron microscopy (HR-TEM). Radioactivities were measured using the gamma counter (Wizard 1470; Perkin Elmer). The mouse was scanned with Inveon SPECT/CT system (Siemens Medical Solutions, Knoxville, TN, USA), equipped with a 1-pinhole mouse high sensitivity collimator.

Results and Discussion

As seen in the Figure 1(b), all the diffraction peaks match well with those of the corresponding standard wurtzite ZnO pattern (*P*6$_3$*mc*, *a* = 3.249 Å, *c* = 5.206 Å, JCPDS No. 36-1451), indicating that the wurtzite CoO nanorod cores were successfully synthesized.[20] In order to characterize the exact structure of the CoO@SiO_2 core–shell nanostructure, we have measured the XRD patterns. Although, XRD intensity of CoO@SiO_2 core-shell nanostructure was decreased after silica coating due to amorphous nature of coating materials, all the diffraction peaks of the pristine CoO nanorods are clearly remained (Figure 1(a)). Based on the above results,

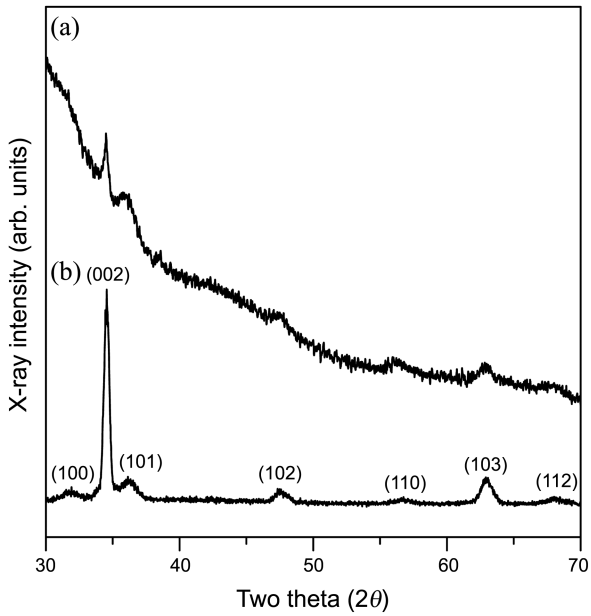

Figure 1. X-ray diffraction patterns (XRD) of (a) CoO@SiO_2 nanoshell and (b) core CoO nanorods, respectively.

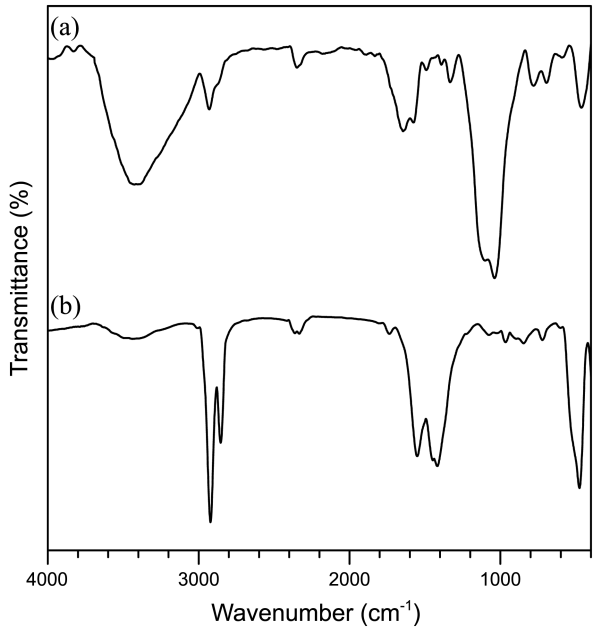

Figure 2. FT-IR spectra of (a) a CoO@SiO_2 core-shell nanoparticle and (b) a core CoO nanorod.

we can conclude that the crystal structure of core CoO nanorods did not change after silica coating.

From the FT-IR spectra of before and after silica coating (Figure 2), the CoO@SiO_2 core-shell nanostructure shows a broad and extensive band in the 3,705-2,994 cm^{-1} corresponding to the O-H stretching vibration of water molecules on the silica shell surface. Whereas, the strong absorption bands at 1,095 cm^{-1} and 1,032 cm^{-1} are the symmetric and asymmetric stretching vibrations of Si-O-Si. The peaks at 2,924 cm^{-1} and 2,852 cm^{-1} are associated with the asymmetric and symmetric CH_2 stretching modes, existing in oleic acid on the surface of core CoO nanorods. Two bands located at 1,551 cm^{-1} and 1,413 cm^{-1} can be assigned to the bidentate coordination of the oleate anion on the CoO core particles surface. In particular, the spectra show an intense peak at 470 cm^{-1} which ascribed to the Co-O vibration modes in the wurtzite CoO core.

Figure 3(a) shows the HR-TEM image of the core CoO nanorods with dimension of 43.6 nm (length) × 6.4 nm (diameter). The size and morphology of the synthesized CoO nanorods are quite uniform (Supporting Information, Figure S1). The inter-rod distance of CoO nanorods was 3-4 nm, which corresponds approximately to two layers of the oleic acid surfactant on the surface of core CoO nanorods. Figure 3(b) displays the silica coated CoO nanorods. The shape and size of core CoO nanorods are clearly remained after silica coating (Supporting Information, Figure S2). The radioactivity of core [^{57}Co]CoO nanorods and [^{57}Co]CoO@SiO_2 core-shell nanostructure were 423 μCi and 118 μCi, respectively. The radiochemical yield of the final [^{57}Co]CoO@SiO_2 core-shell nanostructure was about 12%.

Figure 4 shows the SPECT imaging of the nude mice injected with [^{57}Co]CoO@SiO_2 core-shell nanostructure intravenously. Generally, the radionuclide such as F-18 was

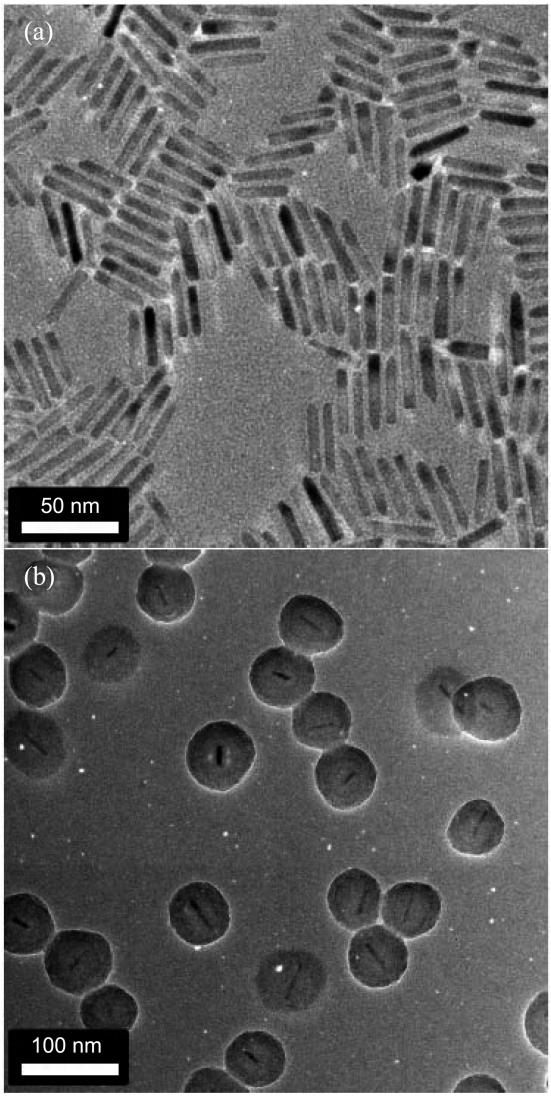

Figure 3. HR-TEM images of (a) core CoO nanorods and (b) CoO@SiO_2 core-shell nanostructure.

accumulated in bladder due to cleavage from conjugated compound and clearance by living system. In this case, however, some different pattern shows that intensity of Co-57 is weak in bladder. This is evidence that [^{57}Co]CoO@SiO_2 core-shell is relatively stable without cleavage. Lung, liver and spleen were the major host organs for the [^{57}Co]CoO@SiO_2 core-shell nanostructure. The SPECT image, which is similar to Kumar's report, showed that nanoparticles were accumulated in the liver and spleen by cells of reticuloendothelial system (RES).[21] It is interesting to note that the radioactivity in the lung was predominantly enhanced comparing to Kumar's report. Kumar *et al.* studied the biodistribution using organically modified silica nanoparticles for fluorescence and positron emission tomography (PET). On the other hand, in this study [^{57}Co]CoO@SiO_2 core-shell was used without any residues on the surface. It shows a different uptake of organ depending on a kind of modified functional group. Moreover, a high accumulation of [^{57}Co]-CoO@SiO_2 core-shell in lung has a potential for use in

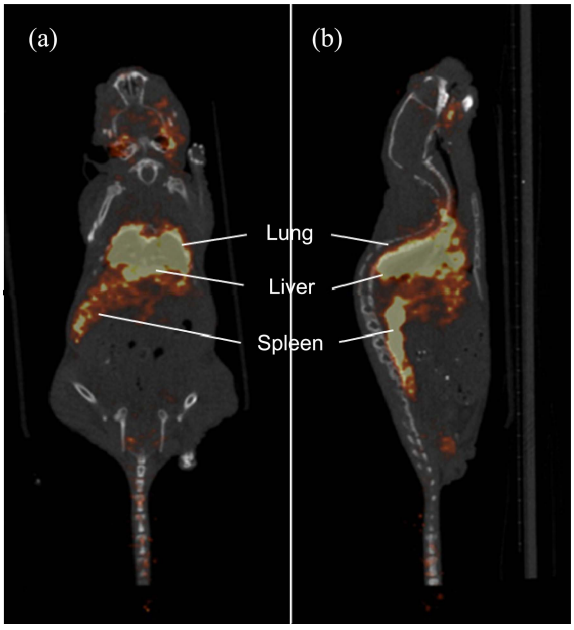

Figure 4. SPECT/CT image of mice injected [^{57}Co]CoO@SiO_2 core-shell nanostructure. (a) whole body sagittal and (b) coronal image.

pulmonary diagnosis and therapy.[22] Another feature in SPECT image is to visualize salivary glands in head of mice. Salivary glands make saliva, which aids in digestion and keeps mouth moist. In fact, salivary gland cancer is a rare form of cancer that begins in the salivary glands.[22] These might have a result in interpolating radionuclide Co-57 into cobalt oxide contrary to imaging probes conjugated nanoparticles.

Conclusion

The cat's eye-shaped [^{57}Co]CoO@SiO_2 core-shell nanostructure was successfully prepared by the thermal decomposition and reverse microemulsion methods. The biodistribution in mice indicated that radiocobaltnuclide inserted nanoparticles have a potential as a novel SPECT imaging agent investigating metabolism compared to imaging probe conjugated nanoparticles. These studies provide preliminary research to the Co-57 radiolabeled nanoparticles for diagnostic applications.

Acknowledgments. This research was supported by Leading Foreign Research Institute Recruitment Program and Basic Science Research Program through the National Research Foundation of Korea (NRF) funded by the Ministry of Education, Science and Technology (MEST) (No. 2013-044975) and the Ministry of Education (No. NRF-2013R1A1A2013035).

Supporting Information. Low-magnification HR-TEM images of core CoO nanorods and CoO@SiO_2 core-shell nanostructures.

References

1. Schober, O.; Rahbar, K.; Riemann, B. *Eur. J. Nucl. Med. Mol. Imaging* **2009**, *36*, 302.
2. Hong, H.; Zhang, Y.; Sun, J.; Cai, W. *Nano Today* **2009**, *4*, 399.
3. Hagooly, A.; Rossin, R.; Welch, M. J. *Handb. Exp. Pharmacol.* **2008**, 93.
4. Welch, M. J.; Hawker, C. J.; Wooly, K. L. *J. Nucl. Med.* **2009**, *50*, 1743.
5. Gunasekera, U. A.; Pankhurst, Q. A.; Douek, M. *Target Oncol.* **2009**, *4*, 169.
6. Sanvicens, N.; Marco, M. P. *Trends Biotechnol.* **2008**, *26*, 425.
7. Villa, C. H.; McDevitt, M. R.; Escorcia, F. E.; Rey, D. A.; Bergkvist, M.; Batt, C. A.; Scheinberg, D. A. *Nano Lett.* **2008**, *8*, 4221.
8. Rojas, S.; Gispert, J. D.; Martin, R.; Abad, S.; Menchon, C.; Pareto, D.; Victor, V. M.; Alvaro, M.; Garcia, H.; Herance, J. R. *ACS Nano* **2011**, *5*, 5552.
9. Pinna, N.; Niederberger, M. *Angew. Chem. Int. Ed.* **2008**, *47*, 5292.
10. Park, J.; Joo, J.; Kwon, S. G.; Jang, Y.; Hyeon, T. *Angew. Chem. Int. Ed*. **2007**, *42*, 4630.
11. Front, D.; Israel, O.; Iosilevsky, G.; Even-Sapir, E.; Frenkel, A.; Peleg, H.; Steiner, M.; Kuten, A.; Kolodny, G. M. *Radiology* **1987**, *165*, 129.
12. Kagadis, G. C.; Loudos, G.; Katsanos, K.; Langer, S. G.; Nikiforidis, G. C. *Med. Phys.* **2010**, *37*, 6421.
13. Park, S. I.; Kwon, B. J.; Park, J. H.; Jung, H.; Yu, K. H. *Nanosci. Nanotechnol.* **2011**, *11*, 1815.
14. Nam, K. M.; Shim, J. H.; Han, D.; Kwon, H. S.; Kang, Y.; Li, Y.; Song, H.; Seo, W. S.; Park, J. T. *Chem. Mater.* **2010**, *22*, 4446.
15. Seo, W. S.; Shim, J. H.; Oh, S. J.; Lee, E. K.; Hur, N. H.; Park, J. T. *J. Am. Chem. Soc.* **2005**, *127*, 6188.
16. Zhang, Y.; Zhu, J.; Song, X.; Zhong, X. *J. Phys. Chem. C* **2008**, *112*, 5322.
17. Xia, B. Y.; Yang, P.; Sun, Y.; Wu, Y.; Mayers, B.; Gates, B.; Yin, Y.; Kim, F.; Yan, H. *Adv. Mater.* **2003**, *15*, 353.
18. Laurent, S.; Forgre, D.; Port, M.; Roch, A.; Robic, C.; Vander Elst, L.; Muller, R. N. *Chem. Rev.* **2008**, *108*, 2064.
19. Cannas, C.; Musinu, A.; Ardu, A.; Orru, F.; Peddis, D.; Caus, M.; Sanna, R.; Angius, F.; Diaz, G.; Piccaluga, G. *Chem. Mater.* **2010**, *22*, 3353.
20. Lokhande, C. D.; Dubal, D. P.; Joo, O. *Current Applied Physics* **2011**, *11*, 255.
21. Kumar, R.; Roy, I.; Ohulchanskky, T. Y.; Lisa, A. V.; Bergey, E. J.; Prasad, P. N. *ACS Nano* **2010**, *23*, 699.
22. Liu, Y.; Welch, M. J. *Bioconjugate Chem.* **2012**, *23*, 671.